Dopant distribution for maximum carrier mobility in selectively doped $Al_{0.30}Ga_{0.70}As/GaAs$ heterostructures

E. F. Schubert, Loren Pfeiffer, K. W. West, and A. Izabelle[a)]
AT&T Bell Laboratories, 600 Mountain Avenue, Murray Hill, New Jersey 07974

(Received 21 November 1988; accepted for publication 30 January 1989)

The magnitude of potential fluctuations due to remote ionized dopants is calculated for selectively doped heterostructures using unscreened and screened Coulomb potentials. Potential fluctuations are found to be minimized (corresponding to maximum carrier mobility) if the dopant distribution is δ-function-like. Our experimental study of electron mobilities in selectively doped heterostructures grown by molecular beam epitaxy reveals that carrier mobility indeed increases as the thickness of the doped layer is reduced, in agreement with the calculation. A peak electron mobility of 5.5×10^6 cm^2/V s is obtained at low temperatures in a selectively δ-doped heterostructure.

The highest electron mobilities for any semiconductor are obtained at low temperatures in selectively doped n-type $Al_xGa_{1-x}As/GaAs$ heterostructures.[1-7] Various doping schemes were used to optimize such heterostructures including homogeneous doping,[3,5,6] single[2,4,7] and multiple[1] delta-doping sheets. The electron mobilities in selectively doped heterostructures were estimated by means of numerical calculations.[8-11] Scattering of electrons by remote ionized dopants located in the $Al_xGa_{1-x}As$ is the dominating scattering mechanism at low temperatures for moderate spacer thicknesses.[12]

In this letter we report the first systematic experimental and theoretical study on the dependence of carrier mobility on the dopant distribution. In the first part we calculate potential fluctuations within the channel region of the selectively doped heterostructure for various dopant distributions chosen to yield the same two-dimensional electron gas concentration. We show that potential fluctuations are minimized (i.e., remote ionized impurity limited mobility maximized) if the doping profile is δ-function-like. In the second, experimental part of this letter we report on Hall mobilities of selectively doped $Al_xGa_{1-x}As/GaAs$ heterostructures with different doping configurations, and compare the trend of the experimental results with our theoretical predictions.

The conduction-band diagrams of two selectively doped heterostructures with different doping configurations are shown in Fig. 1. The doped region has a thickness of z_d and its centroid is at a distance of z_c from the heterointerface. The doping configurations shown in Fig. 1 are represented by the doping profile

$$N_D(z) = N_D^{2D}/z_d\{\sigma[z-(z_c-\tfrac{1}{2}z_d)] - \sigma[z-(z_c+\tfrac{1}{2}z_d)]\}, \qquad (1)$$

where the thickness z_d is a free parameter, $N_D^{2D}/z_d = N_D$ is the three-dimensional (3D) doping concentration in the doped layer, and $\sigma(z)$ is the step function. One can easily verify that the doping profiles given in Eq. (1) result in the same electric displacement and potential at the heterointerface for different z_d. Thus, Eq. (1) provides different doping configurations but identical free-carrier concentrations: $N_D^{2D} = n_{2DEG} =$ const. Note that as z_d increases the undoped $Al_xGa_{1-x}As$ spacer layer $(z_c - z_d/2)$ decreases, and simultaneously the 3D doping concentration N_D^{2D}/z_d is reduced. The trend of the mobility is, therefore, not obvious as z_d is changed. Present mobility calculations do not take into account the randomness of the impurity distribution. Furthermore, in the mobility calculations the total impurity potential is taken as the relevant scattering potential. However, it would be more appropriate to use only the smaller amplitude of the potential fluctuation as the scattering potential. An analytic approximation for the dependence of the electron mobility on the design parameters of the heterostructure has been proposed.[9] However, subsequent work of the author showed that the exact functional dependences are yet to be determined.[9]

Next, we determine the magnitude of potential fluctuations at the interface due to random impurity distribution within the doped layer. First, we calculate potential fluctuations analytically using unscreened Coulomb potentials. Subsequently, we calculate potential fluctuations numerically using screened Coulomb potentials. As shown in Fig. 2 the volume element dV_i contains a mean total number of dopant

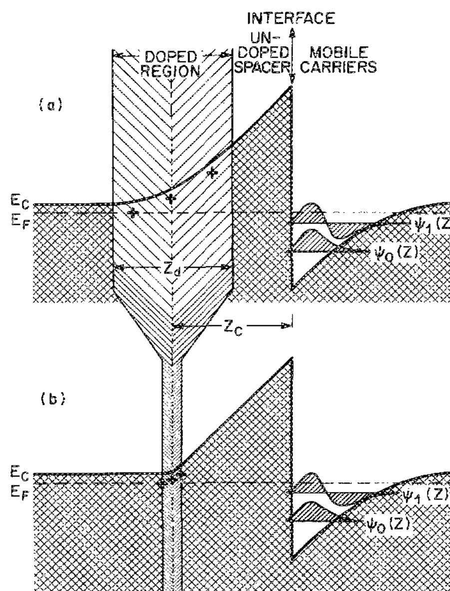

FIG. 1. Schematic illustration of the conduction-band diagram of a selectively doped heterostructure for different doped layer thicknesses and doping concentrations. The free-carrier density remains constant upon changing the doped layer thickness.

[a)] AT&T Bell Laboratories, Holmdel, New Jersey 07733.

 0003-6951/89/141350-03$01.00 © 1989 American Institute of Physics

Downloaded 14 Jul 2003 to 128.113.111.105. Redistribution subject to AIP license or copyright, see http://ojps.aip.org/aplo/aplcr.jsp

atoms of $N = N_D\, dV$. N varies from unit volume to unit volume due to statistical dopant distribution. The charge-density fluctuation causes a potential fluctuation at the plane of the heterointerface. The statistical variance of the potential fluctuation at the interface caused by one unit volume located at (r,α,z) can be obtained using Poisson statistics. Using unscreened Coulomb potentials for the impurities yields for the variance of potential fluctuations

$$d\sigma_\phi^2 = (e/4\pi\epsilon)^2 N_D\, dr\, r d\alpha\, dz (r^2 + z^2)^{-1}, \tag{2}$$

where e is the elementary charge, $dr\, rd\alpha\, dz$ is the unit volume dV_i in cylindrical coordinates as shown in Fig. 2, and ϵ is the permittivity of the semiconductor. The total mean potential fluctuation at the interface is obtained by integration over the entire doped layer

$$\sigma_\phi^2 = \int_z \int_r \int_\alpha d\sigma_\phi^2 . \tag{3}$$

We restrict our calculation to charge fluctuations occurring within a screening radius r_s. One obtains for $z_c \ll r_s$

$$\sigma_\phi^2 = 2\pi \frac{N_D^{2D}}{z_d} \left(\frac{e}{4\pi\epsilon}\right)^2 \left[\left(z_c - \frac{z_d}{2}\right)\left(\ln \frac{z_c - z_d/2}{r_s} - 1\right) - \left(z_c + \frac{z_d}{2}\right)\left(\ln \frac{z_c + z_d/2}{r_s} - 1\right)\right] \tag{4}$$

and for $z_c \gg r_s$

$$\sigma_\phi^2 = \pi N_D^{2D} (e/4\pi\epsilon)^2 r_s^2 / (z_c^2 - \tfrac{1}{4} z_d^2). \tag{5}$$

We now minimize the variance of the potential fluctuation with respect to the thickness of the doped layer. Calculating $\partial\sigma_\phi^2/\partial z_d = 0$ for Eq. (4) and Eq. (5) yields that σ_ϕ^2 is minimized, if $z_d \to 0$, that is if the doped layer thickness approaches zero. The doping profile is then given by the δ function[13,14]:

$$N_D(z) = N_D^{2D} \delta(z + z_c). \tag{6}$$

The minimum standard deviation of the potential is for $z_c \ll r_s$ given by

$$\sigma_\phi = (e/4\pi\epsilon) \{2\pi N_D^{2D} [1 - \ln(z_c/r_s)]\}^{1/2} \tag{7}$$

and for $z_c \gg r_s$

$$\sigma_\phi = (e/4\pi\epsilon)(\pi N_D^{2D})^{1/2} r_s / z_c. \tag{8}$$

With a two-dimensional (2D) screening radius given by[10]

$$r_s = (2\epsilon/e^2)(\pi\hbar^2/m^*) \cong 52\ \text{Å}, \tag{9}$$

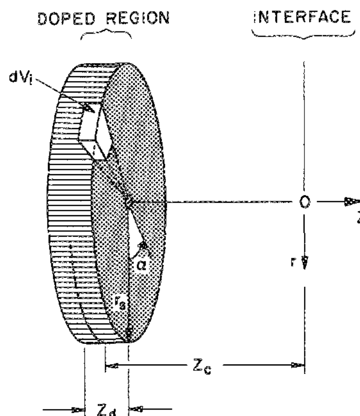

FIG. 2. Doping configuration used to calculate potential fluctuations at the heterointerface resulting from statistical dopant distribution in the doped layer.

where $\hbar$ is Planck's constant divided by 2π and m^* is the effective electron mass. As an example, for $z_c = 500$ Å and $N_D^{2D} = 1\times 10^{12}$ cm^{-2} one obtains from Eq. (8) a mean potential fluctuation of $\sigma_\phi \cong 2$ mV.

The employment of screened Coulomb potentials rather than unscreened potentials refines the above calculation. The Coulomb potential of an impurity located at (r,z) screened by electrons which are assumed to be in the plane $z=0$ is given by[10]

$$\phi(r,z) = \int_0^\infty qA(q) J_0(qr) dq, \tag{10}$$

where J_0 is the Bessel function of zero order and

$$A(q) = \frac{e}{4\pi\epsilon} \frac{e^{-qz}}{q + 1/r_s}. \tag{11}$$

For large r, the Coulomb potential screened by a 2D sheet of electrons follows the proportionality

$$\phi(r,z) \sim 1/r^3 \tag{12}$$

and decays more rapidly than the unscreened Coulomb potential. The screened Coulomb potential is obtained by a numerical integration of Eq. (10) and then inserted in Eq. (2). However, the minimization of potential fluctuations is still achieved, if the doped layer thickness approaches zero.

The minimization of potential fluctuations is equivalent to a maximization of remote ionized impurity mobility, since the scattering matrix element is proportional to the magnitude of the scattering potential. Thus, the electron mobility and the magnitude of potential fluctuations obey a monotonical relationship, which is valid even in the presence of screening.

The $Al_{0.30}Ga_{0.70}As$/GaAs epitaxial layers were grown by molecular beam epitaxy in a modified Varian Gen II system on semi-insulating ⟨100⟩ oriented GaAs substrates. The layer sequence consists of an undoped GaAs/$Al_{0.30}Ga_{0.70}As$ superlattice buffer, a 1.0-μm-thick GaAs channel layer, a partially Si-doped $Al_{0.30}Ga_{0.70}As$ (5740 Å) layer, and an undoped GaAs (100 Å) top layer. The $Al_{0.30}Ga_{0.70}As$ contains two doped regions.[15] The centroid of the surface doped region accounts for surface depletion and is located 150 Å before the $Al_{0.30}Ga_{0.70}As$ growth is terminated. The surface doped region consists of four δ-doped sheets with $N_D^{2D} = 5.0\times 10^{11}$ cm^{-2} separated by 60 Å. The thickness of the doped layer close to the interface was systematically varied between $z_d \to 0$ Å and $z_d = 800$ Å in a pseudorandom sample sequence. The centroid of the doped region was kept constant at $z_c = 500$ Å from the interface. The total 2D dopant concentration was also kept constant $N_D^{2D} = 5.0\times 10^{11}$ cm^{-2}. For improved parameter control, 10 δ-doped sheets each with $N_D^{2D} = 5\times 10^{10}$ cm^{-2} separated by $z_d/9$ were employed.

Experimental Hall mobilities μ (left ordinate) and carrier concentrations n_{2DEG} (right ordinate) of the samples are shown in Fig. 3. The thickness of the doped layer is changed as illustrated in the inset. The electron mobilities at 4.2 K range between 860 000 cm^2/V s for $z_d = 800$ Å and 4.53×10^6 cm^2/V s for $z_d \to 0$ Å. Mobilities are measured in the dark after illumination. Electron mobilities clearly increase as z_d decreases as shown in Fig. 3 with the highest

Downloaded 14 Jul 2003 to 128.113.111.105. Redistribution subject to AIP license or copyright, see http://ojps.aip.org/aplo/aplcr.jsp

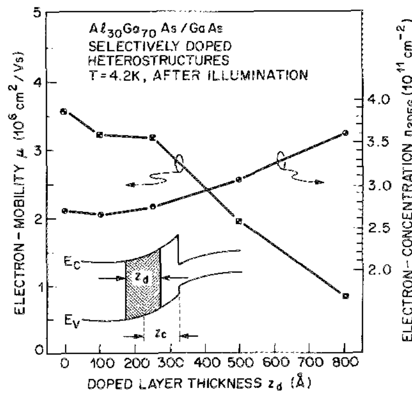

FIG. 3. Electron mobility (left ordinate) and electron density (right ordinate) vs doped layer thickness of selectively doped heterostructures grown by molecular beam epitaxy. The samples are grown sequentially with $z_d = 0$, 500, 250, 800, 100, and 0 Å, respectively. This displayed value for $z_d \to 0$ Å represents an average value. The densities and mobilities measured before illumination are typically 15–35% lower but follow the same qualitative trend.

mobility obtained as z_d approaches zero. The mobility follows the qualitative trend predicted by the theoretical model. At small thicknesses of the doped layer, only minor changes of the mobility are expected: Eq. (5) shows that the change of the scattering potential becomes negligible as z_d approaches zero (i.e., $d\sigma_\phi/dz_d = 0$ for $z_d \to 0$). We indeed observe such a weak dependence of the mobility on z_d as $z_d \to 0$.

Figure 3 further illustrates the carrier density as a function of the doped layer thickness. An increase of n_{2DEG} is observed as z_d increases, which is not expected if only shallow donors are taken into account. A probable cause for this increase is the coexistence of shallow and deep donors in the $Al_xGa_{1-x}As$[16]: As z_d increases, more deep donors are elevated above the Fermi level in the doped region close to the interface as illustrated in Fig. 1. Consequently, the deep donors nearest the interface become ionized and the mobile carrier density is enhanced. This concentration enhancement is expected for carriers in the dark. It is apparently maintained even after illumination in samples with large z_d, due to photoionization of deep donors closer to the interface.

In addition to remote donors in the $Al_xGa_{1-x}As$, unintentional shallow and deep impurities in the vicinity of the interface reduce the carrier mobility. The influence of any such static imperfection is reduced by screening. The mobility increases with concentration due to screening following the relation $\mu \sim n_{2DEG}^{\beta}$ with $0.5 \leqslant \beta \leqslant 1.5$. Thus, the decrease of mobility with increasing z_d (see Fig. 3) would be even more pronounced, if n_{2DEG} were independent of z_d.

The electron mobility of the highest mobility sample grown in the present series is shown in Fig. 4 for temperatures $4.2\ K \leqslant T \leqslant 300\ K$. The mobility is measured in the dark (closed circles) and after illumination (open circles). At $T = 0.3$ K the mobility is $5.5 \times 10^6\ cm^2/V\,s$ with $n_{2DEG} = 2.6 \times 10^{11}\ cm^{-2}$. Even higher mobilities are achieved in our molecular beam epitaxy system with increased z_c.[7] Since the 0.3 K mobilities approximately track the 4.2 K mobilities for the samples investigated here, the 4.2 K mobilities are indicative of the residual very low temperature mobility in which ionized impurity scattering plays an important role.

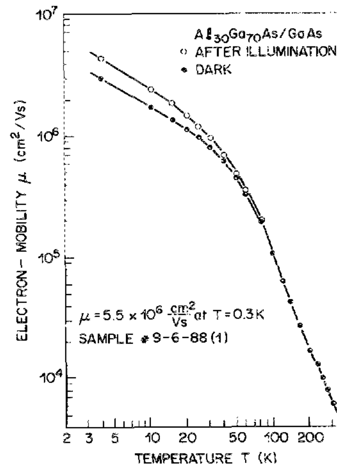

FIG. 4. Electron mobility as a function of temperature for a selectively doped heterostructure. The doped region consists of a single δ-doped sheet separated by 500 Å from the $Al_{0.30}Ga_{0.70}As$/GaAs interface.

In conclusion, we investigated the role of dopant distribution in selectively doped heterostructures. Statistical potential variations at the heterointerface due to random dopant distribution are calculated using unscreened Coulomb potentials and Coulomb potentials screened by a 2D sheet of carriers. It is shown that ionized impurity mobility is maximized if the thickness of the doped layer approaches zero. Experimental electron mobilities in selectively doped heterostructures with different doped layer thicknesses show a clearly increasing electron mobility, as the doped layer thickness decreases. A low-temperature mobility of $5.5 \times 10^6\ cm^2/V\,s$ is obtained in a selectively δ-doped heterostructure.

The authors thank T. Y. Chang, J. E. Cunningham, L. C. Feldman, and H. L. Störmer for valuable discussions during the course of this work. We thank K. W. Baldwin for magnetotransport measurements at $T = 0.3$ K. The MBE growers L. N. P. and K. W. W. especially thank A. C. Gossard and J. E. English for their patient tutoring in the art of high-mobility MBE crystal growth.

[1] J H. English, A. C. Gossard, H. L. Störmer, and K. W. Baldwin, Appl. Phys. Lett. **50**, 1826 (1987).
[2] J. E. Cunningham, W. T. Tsang, G. Timp, E. F. Schubert, A. M. Chang, and K. Owusu-Sekyere Phys. Rev. B **37**, 4317 (1988).
[3] E. E. Mendez, P. J. Price, and M. Heiblum, Appl. Phys. Lett. **45**, 294 (1984).
[4] M. Shayegan, V. J. Goldman, C. Jiang, T. Sajoto, and M. Santos, Appl. Phys. Lett. **52**, 1086 (1988).
[5] C. T. Foxon, J. J. Harris, W. G. Wheeler, and D. E. Lackison, J. Vac. Sci. Technol. B **4**, 511 (1986).
[6] K. Hiyamizu, J. Salto, K. Nanbu, and T. Ishikawa, Jpn. J. Appl. Phys. **22**, 1609 (1983).
[7] Loren Pfeiffer, K. W. West, H. L. Störmer, and K. W. Baldwin (unpublished).
[8] W. Walukiewicz, H. E. Ruda, J. Lagowski, and H. C. Gatos, Phys. Rev. B **30**, 4571 (1984).
[9] P. J. Price, J. Vac. Sci. Technol. **19**, 599 (1981); Surf. Sci. **113**, 199 (1982); Surf. Sci. **134**, 145 (1984).
[10] T. Ando, A. B. Fowler, and F. Stern, Rev. Mod. Phys. **54**, 437 (1982).
[11] T. Ando, J. Phys. Soc. Jpn. **51**, 3893 (1982); **51**, 3900 (1982).
[12] H. L. Störmer, A. Pinczuk, A. C. Gossard, and W. Wiegmann, Appl. Phys. Lett. **38**, 691 (1981).
[13] E. F. Schubert, J. B. Stark, B. Ullrich, and J. E. Cunningham, Appl. Phys. Lett. **52**, 1508 (1988).
[14] E. F. Schubert, J. E. Cunningham, W. T. Tsang, and G. L. Timp. Appl. Phys. Lett. **51**, 1170 (1988).
[15] B. Etienne and E. Paris, J. Phys. (Paris) **48**, 2049 (1987).
[16] E. F. Schubert and K. Ploog, Phys. Rev. B **30**, 7021 (1984).

Downloaded 14 Jul 2003 to 128.113.111.105. Redistribution subject to AIP license or copyright, see http://ojps.aip.org/aplo/aplcr.jsp